# Single-Atom Test of All-Atom Empirical Potentials: Fe in Myoglobin

**Brajesh K. Rai, Earl W. Prohofsky, and Stephen M. Durbin***

*Department of Physics, Purdue University, West Lafayette, Indiana 47907*

*Received: June 2, 2005; In Final Form: August 11, 2005*

The measured Fe vibrational density of states in deoxy-myoglobin, obtained from nuclear resonance vibrational spectroscopy, is compared to results from a normal-mode analysis using an all-atom empirical potential. Substantial disagreement reveals that for this one atom, the empirical potential does not accurately describe the actual forces. A Green function technique is developed to calculate the iron vibrational spectrum of deoxy-myoglobin by coupling the independently calculated heme and globin normal modes; nonbonded interactions between the heme molecule and the protein are essential for a good fit to the measurements. A projection of the eigenvectors from this potential onto the displacements induced by binding of CO demonstrates that normal modes over a broad range centered around 50−150 $cm^{-1}$ may drive the ligand-induced structural changes.

## I. Introduction

Computer simulations are widely used to model the dynamics of proteins and other complex macromolecules.[1−4] Many are based on empirical, all-atom potentials that approximate the true, many-body potential with a parametrized function describing the forces on each individual atom. The parameters of an all-atom potential are force constants and nonbonded interactions (e.g., Lennard-Jones and electrostatic forces) between a given atom and its neighbors that largely depend on their chemical identities and the structural arrangement. Improving the reliability of these simulations is of great interest, as they are being applied to increasingly large and complex macromolecular systems. The fundamental question for any empirical potential, however, is whether the set of force constants is accurate enough to predict collective motions that are physically realized.

Force constants and nonbonded interactions for various atoms are deduced from measured and calculated physical properties of a relatively small number of model molecules that are similar to the building blocks of biological macromolecules, e.g., the amino acid residues of proteins. A particularly thorough description of constructing, optimizing, and validating the all-atom CHARMM potential is found in MacKerell et al.,[1] which gives the explicit potential energy function and strategies for optimizing the parameters using experimental data such as Raman spectroscopy from model compounds and results of ab initio calculations. Other critical issues include the treatment of dielectric response, nonbonded interactions, and procedures for determining the best value of a parameter. The empirical potential is used for the full molecular dynamics simulation in femtosecond steps over times ranging up to a few nanoseconds. The ensemble of calculated molecular configurations is used to compute, for example, the root-mean-square (rms) difference in the backbone from the crystallographic structure, its radius of gyration, and especially the rms fluctuations of each residue. This last term is compared to X-ray crystallographic data for the Debye−Waller B factors describing thermal motion of the residues; good agreement has been reported.[1]

Assessing an empirical potential with thermal B factors illustrates the problematic nature of validating these simulations. Thousands of individual parameters are built into a program, but only time-averaged output is compared to a few hundred data points describing average thermal motions of the set of residues. While it is necessary for a useful molecular dynamics program to get the rms values right, it likely is not always sufficient. The difficult question of how to reliably validate such potentials is beyond the scope of this paper, but we do address a more limited question: Are the force constants correct for one particular atom? For the single Fe atom in myoglobin, we compare the partial vibrational density of states (VDOS) projected out from the CHARMM normal mode spectrum with the measured Fe VDOS determined from nuclear resonance vibrational spectroscopy (NRVS).[5] Significant disagreement is observed, indicating that heme Fe dynamics are not being accurately described.

Unlike the heme model compounds, where force field refinements lead to a good agreement between calculation and the experimental NRVS data, the large size of the proteins makes it impractical to iteratively perform the normal-mode analysis and refine the calculation to the experimental data. We develop an alternative Green-function-based approach to calculate the Fe vibrational spectrum of deoxy-myoglobin by coupling the normal modes of the isolated heme and globin subunits of the system. This approach keeps the globin normal modes from CHARMM unchanged, but adjusts the local potential for the heme molecule and its couplings to the protein. Good agreement is obtained with suitable adjustment of nonbonded interactions between the heme and the globin. This approach is used to explore the modes that couple deoxy-myoglobin to (carbon monoxy)-myoglobin, providing insight into the dynamics of ligand binding to myoglobin.

## II. Deoxymyoglobin normal Modes

We performed a standard normal-mode analysis of deoxy-myoglobin (DMb) using CHARMM. The starting point was an X-ray structure for DMb from the Protein Data Bank (1BZP).[6,7] The initial structure, which includes water molecules, was put through an energy minimization process using CHARMM22

* Corresponding author: tel, 765 494-6426; fax, 765 494-0706; e-mail, durbin@physics.purdue.edu.

10.1021/jp052950i CCC: $30.25 
Published on Web 09/20/2005

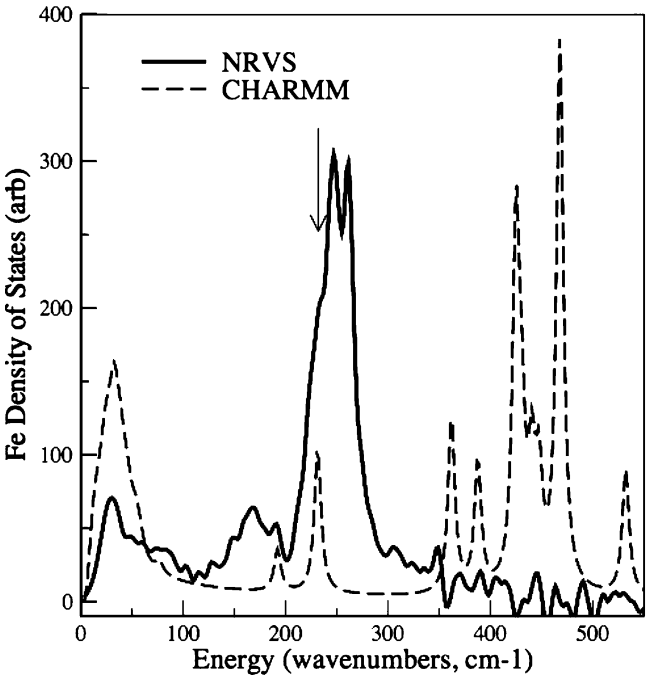


**Figure 1.** Fe vibrational density of states determined from nuclear resonance vibrational spectroscopy (NRVS) measurements (solid line) and projected out from a CHARMM normal mode calculation (dashed line). The two spectra have been normalized to have equal areas, after applying the experimental resolution function of 8 $cm^{-1}$ to the calculated spectrum. The arrow near 220 $cm^{-1}$ denotes the expected Fe−His stretch mode, seen as a shoulder in the NRVS results and a peak in the CHARMM output.

force fields. Default parameter values were used to treat Lennard-Jones and Coulomb interactions. The energy minimization process involved 2000 steps of steepest descent method, followed by 1000 steps of conjugate gradient method. The resulting Hessian matrix was diagonalized to give normal modes of the system.[8] The six lowest eigenvalues, corresponding to the translational and rotational degrees of freedom, are very close to zero ($<10^{-4}$), indicating a good convergence of minimization procedure. The Fe displacement corresponding to each normal mode was extracted from the eigenvectors of the system, and from these we calculated the Fe VDOS.[9−11]

The measured VDOS for Fe in DMb obtained by nuclear resonance vibrational spectroscopy was determined from the data published by Sage et al.,[12] using the standard analysis package.[13] NRVS is a synchrotron-based X-ray spectroscopy where the absorption probability for X-ray energies near the Mössbauer resonance depends on the vibrational density of states of the $^{57}$Fe nuclei. The experimental procedures and theory underpinning this fairly new technique have been extensively discussed elsewhere.[14−24] Note that all NRVS modes are due exclusively to Fe motion and that all Fe modes of significant amplitude are detected as there are no optical selection rules to limit its sensitivity. Furthermore, accurate knowledge of the nuclear scattering cross section and application of sum rules[13,25] allows quantitative determination of mode amplitudes, without the uncertainties due to unknown matrix elements that affect peak intensities in resonance Raman and infrared vibrational spectroscopies.

The CHARMM prediction is compared to the NRVS measurement of the VDOS in Figure 1; significant disagreement is immediately apparent. Both traces show a "protein peak" near 25 $cm^{-1}$, so-called because inelastic neutron scattering shows similar dynamics of the protein backbone in this region.[26,27] The CHARMM trace also shows a well-defined peak near 220 $cm^{-1}$, the location of a well-studied Raman line corresponding to a stretching motion between the Fe atom and the imidazole ring of the histidine residue that binds the heme to the protein.[28] This shows up in the NRVS spectrum as just a shoulder on a much larger structure due to in-plane modes, which are not Raman-active and had never been seen before the NRVS data became available. (We note that Melchers et al. did a similar simulation[29] where they reported on a subset of the Fe motion perpendicular to the heme plane and also found a peak near this Raman line; they did not report results for in-plane modes.)

Much of the spectral weight predicted by this simulation occurs at higher frequencies, where the data show little or no intensity. This corresponds to the average force on Fe in CHARMM being significantly larger than the NRVS result.[25] For this single atom comparison, one must conclude that the all-atom empirical potential fails to predict most of the details of the normal mode spectrum and also does not accurately represent the zero-order properties of the true potential.

### III. Refining the Empirical Potential to NRVS Data

While the aim of empirical potentials is to describe all proteins, our immediate goal is to refine the CHARMM potential to the Fe VDOS in DMb. The usual iterative procedure of making a small modification of the potential and comparing the new output to the measured VDOS may not be practical because the many iterations of CHARMM would require a great deal of time and computational resources. We have instead developed a Green function approach to more efficiently calculate the protein's total normal mode spectrum by coupling the independently computed normal modes of the isolated heme and globin subunits of the protein and refine to the measured Fe VDOS by varying the coupling between these subunits. Good agreement is achieved with much shorter computer times and better physical insight because only the heme−globin coupling constants are involved in the refinement computations.

The dynamical eigenvalue equation for the uncoupled, noninteracting heme and globin can be written as[30,31]

$$[M - \omega_0^2 I]q_0 = 0 \tag{1}$$

where $\omega_0$ values are the eigenfrequencies, $q_0$ values are the eigenfunctions, and $I$ is the identity matrix. $M$ is the force constant matrix in mass-weighted Cartesian coordinates and can be expressed as

$$M = \begin{bmatrix} M_h & 0 \\ 0 & M_g \end{bmatrix} \tag{2}$$

where $M_h$ and $M_g$ are the force constant matrixes for the uncoupled heme and globin, respectively. $M_g$ will simply be taken from the CHARMM empirical potential; $M_h$ is available from previous refinements of force fields to NRVS results from several heme model compounds. Heme−globin coupling can be represented by additional terms $C$ in the dynamical equation

$$[M + C - \omega^2 I]q = 0 \tag{3}$$

where $\omega$ and $q$ are eigenvalues and eigenfunctions for the coupled system. The matrix $C$ corresponds to replacing a select number of null terms in eq 2 with coupling parameters between specific atoms of the heme and the globin. Finally, we introduce the Green function matrix $G$

$$G(M - \omega^2 I) = I \tag{4}$$

whose elements are

$$G_{ij}(\omega^2) = \sum_{\omega_0} \frac{q_i^{\omega_0} q_j^{\omega_0}}{({\omega_0}^2 - \omega^2)} \qquad (5)$$

$$\omega^2 \neq {\omega_0}^2$$

This Green-function approach assumes that the eigenvalue problem for the independent heme and globin (eq 1) has already been solved. The assumption that the heme couples to the globin only through a relatively small number of interactions between heme atoms and globin atoms means that the coupling matrix $C$ is sparse. It is then possible to reorder the degrees of freedom so that the matrix $C$ has the form

$$C = \begin{pmatrix} 0 & 0 \\ 0 & C' \end{pmatrix} \qquad (6)$$

The number of variables in the original problem is $3N$, where $N$ is the number of atoms in the heme plus globin system. Equation 6 allows this to be reduced to $3n$, where $n$ is the number of bonds or interactions that couple the heme to the globin. The 9621 variables in the CHARMM simulation for DMb are reduced in this manner to a coupling matrix with only 141 degrees of freedom. Iterative refinement of the coupling constants to the measured VDOS then becomes a routine matter on readily available computers.

The eigenfrequencies and eigenvectors of the globin modes were taken from the CHARMM calculation of DMb, described above. Our model for the heme subunit consists of the protoporphyrin-IX molecule plus the imidazole group from the His93 residue.[32] The heme normal modes were obtained by standard normal-mode analysis using the refined force fields from an earlier study of a porphyrin−imidazole compound.[33] The heme−globin coupling is defined through one covalent and 29 nonbonded interactions, which include all heme−globin atom pairs within a distance of 3.7 Å. The nonbonded interactions were modeled using a Hookean pairwise potential (between atoms a and b)

$$E(r_a, r_b) = \frac{1}{2} k(|r_{a,b}| - |{r_{a,b}}^0|)^2 \qquad (7)$$

where $|r_{a,b}|$ denotes the distance between atoms a and b and superscript 0 represents the given initial configuration. The strength of the potential $k$ is distance dependent, and it decays as $1/r^6$. (A full list of the atoms involved in the heme−globin coupling and their interaction constants is included as Tables 1 and 2 in the Supporting Information. Also included are the coordinates and the force constants used to compute the heme normal modes.) The best-fit result is shown in Figure 2.

Agreement with the doublet of in-plane modes at 250 $cm^{-1}$ and out-of-plane Fe−His mode near 220 $cm^{-1}$, in agreement with previous measurements,[12,28,34] was achieved largely by adjusting the force constants for the uncoupled heme itself. Because these are modes with large Fe amplitudes at relatively high energies, they are well-localized in the heme molecule and show little overlap with globin modes near these frequencies; adjusting the heme−globin force constants had little impact on these modes. At lower frequencies, however, the couplings through the nonbonded interactions were crucial for improving the fit. The protein peak near 25 $cm^{-1}$ includes many modes with large-amplitude translational motions of the heme group, with relatively small motions of the Fe with respect to the porphyrin molecule.

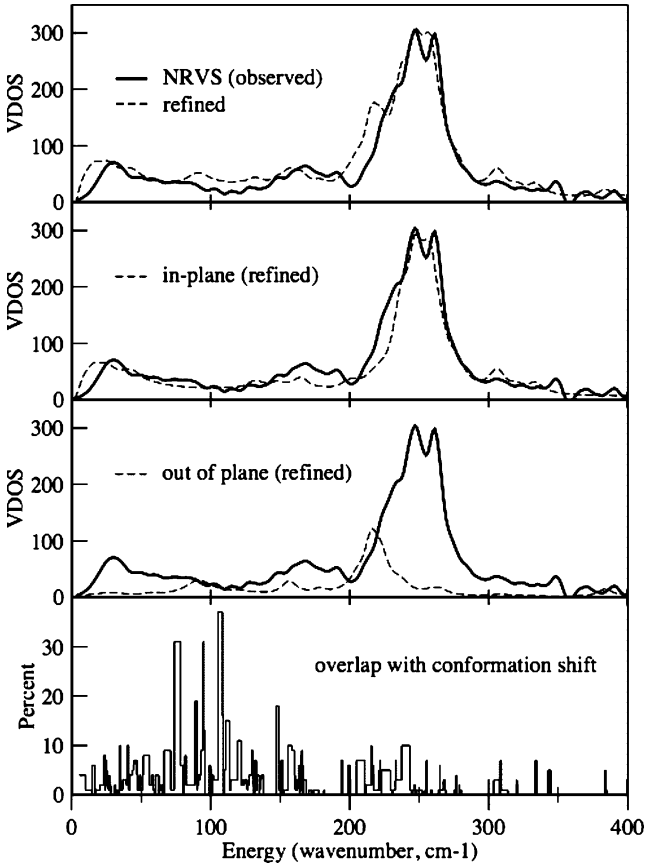


**Figure 2.** Fit of refined potential (dashed line) to the experimental vibrational density of states (solid line). The CHARMM solutions to the globin dynamical equations are combined with results from the heme force field by means of heme−globin coupling constants, which were optimized to produce a good fit. Top panel shows the total refined VDOS; second and third panels display the calculated in-plane and out-of-plane modes, respectively. Bottom panel shows the frequency-dependent overlap of the best-fit eigenvectors with the displacement vector coupling the unligated DMb and ligated MbCO structures, revealing a broad range of modes that can drive this transition.

The intermediate frequency region shows no sharp features, but a broad continuum is clearly visible in the fit and the data. There are numerous out-of-plane modes that originate from similar modes of the isolated heme subunit. Previous studies on heme model compounds also show modes that involve large Fe out-of-plane displacements and significant overlap with the heme doming coordinate.[33,35,36] When put in the protein environment, the heme doming modes couple to large-scale globin vibrations of similar frequencies. Many delocalized protein modes with small Fe fluctuations are found, as opposed to a single, dominant doming mode. This suggests that the effect of the protein on ligand binding to heme, which is accompanied by a perpendicular displacement of the Fe and hence participation of normal modes with this character, is to take the well-resolved doming-like modes of the model heme compounds and broaden them into a nearly continuous distribution by coupling to delocalized globin modes.

## IV. Application to Ligand Binding

The Green function refinement has produced a modified potential that is essentially the same as the CHARMM potential for nearly all of the globin, with little change for the vast majority of globin modes that have negligible overlap with the Fe atom. The potential for the heme unit is based on prior refinements to NRVS data for model heme compounds, and

we have added additional heme−globin coupling terms that were adjusted to produce a good fit to the measured Fe VDOS. Since this should describe Fe dynamics in myoglobin more accurately, we apply it to the binding of CO to form (carbon monoxy)-myoglobin (MbCO).

We consider the overlap between the calculated eigenvectors and a reference vector corresponding to the deoxy to carbon monoxy conformation change transition upon CO binding in Mb, which was constructed from the X-ray crystallography data.[6] This reference vector is only a simple approximation to the actual (unknown) transition path, but it should provide some indication of which modes in the initial DMb configuration play a significant role in initiating the binding process. This reference vector approach has been the basis of various dynamical analyses.[37−40]

As shown in Figure 2, the overlap between the calculated modes and the reference vector is largest for half a dozen modes in the intermediate frequency region, although there is still significant spectral weight at low frequencies and, to a lesser degree, at higher frequencies. Previous normal mode calculations, which were not refined to measurements, suggested that the conformation path from deoxy to ligated states of myoglobin proceeds via a few delocalized modes under 20 $cm^{-1}$,[41] a result not consistent with the Green function analysis of the NRVS data. Instead there is a broad spectrum of protein modes at intermediate frequencies with doming character, and any of these doming-like protein vibrations can be involved in the conformational transition between deoxy and ligated Mb.

Further insight might be obtained by repeating the entire heme−globin normal-mode analysis for the endpoint of this transition, refining the spectrum to NRVS data for MbCO. The heme force field used for DMb was based on the five-coordinated porphyrin−imidazole compound Fe(TPP)(2-MeImH),[33] yet proved to be a good starting point for the protoporphyrin-IX complex in DMb. This same force field might well be adaptable to the MbCO refinement, but starting instead with a force field from an Fe porphyrin compound with a CO ligand, e.g., Fe(TPP)(CO)(1-MeIm),[36] should be more efficient. By analyzing a large enough set of heme model compounds and also refining to different heme proteins, it should be possible to create a generalized empirical potential for the various heme configurations found in heme proteins.

## V. Conclusions

Direct comparison with experiment shows that the CHARMM all-atom empirical potential does not predict the observed dynamics of the Fe atom in deoxy-myoglobin. A Green function technique has been implemented that efficiently allows for refinement of the potential to get good agreement with the NRVS data; this method avoids the recalculation of modes that have negligible overlap with the Fe atom, while focusing on the coupling constants between the heme and the globin. This refined potential for DMb was applied to determining the distribution of modes that couple most strongly the transition from unligated DMb to ligated (carbon monoxy)-myoglobin. A broad distribution is found to be important, especially modes in the range of 50−150 $cm^{-1}$, in contrast to previous predictions suggesting modes at much lower frequencies.

We have demonstrated a method for incorporating experimental data for a single Fe atom into an all-atom empirical potential for deoxy-myoglobin. This approach can be applied to other Fe-containing proteins. One may hope to construct from such efforts a single, parametrized function that would accurately describe the dynamics of at least the Fe atoms for many heme proteins, a modest step toward improving all-atom empirical potentials.

**Acknowledgment.** This work was supported by the National Science Foundation through Award No. PHY-9988763, and the Mobil Manufacturers Forum. B.K.R. acknowledges support of the Purdue Research Foundation.

**Supporting Information Available:** Listings of coordinates and force constants used to compute the heme normal modes and tables of atoms involved in heme−globin coupling and their interaction constants. This material is available free of charge via the Internet at http://pubs.acs.org.

## References and Notes

(1) MacKerell, A. D.; Bashford, D.; Bellott, M.; Dunbrack, R. L.; Evanseck, J. D.; Field, M. J.; Fischer, S.; Gao, J.; Guo, H.; Ha, S.; Joseph-McCarthy, D.; Kuchnir, L.; Kuczera, K.; Lau, F. T. K.; Mattos, C.; Michnick, S.; Ngo, T.; Nguyen, D. T.; Prodhom, B.; Reiher, W. E.; Roux, B.; Schlenkrich, M.; Smith, J. C.; Stote, R.; Straub, J.; Watanabe, M.; Wiorkiewicz-Kuczera, J.; Yin, D.; Karplus, M. *J. Phys. Chem. B* **1998**, *102*, 3586.

(2) Kale, L.; Skeel, R.; Bhandarkar, M.; Brunner, R.; Gursoy, A.; Krawetz, N.; Phillips, J.; Shinozaki, A.; Varadarajan, K.; Schulten, K. *J. Comput. Phys.* **1999**, *151*, 283.

(3) Cornell, W. D.; Cieplak, P.; Bayly, C. I.; Gould, I. R.; Merz, K. M.; Ferguson, D. M.; Spellmeyer, D. C.; Fox, T.; Caldwell, J. W.; Kollman, P. A. *J. Am. Chem. Soc.* **1995**, *117*, 5179.

(4) Brooks, C. L.; Karplus, M.; Pettitt, B. M. *Proteins: a theoretical perspective of dynamics, structure, and thermodynamics*; J. Wiley: New York, 1988.

(5) W. Robert Scheidt, S. M. D.; Sage, J. T. *J. Inorg. Biochem.* **2005**, *99*, 60.

(6) Kachalova, G. S.; Popov, A. N.; Bartunik, H. D. *Science* **1999**, *284*, 473.

(7) Berman, H. M.; Bhat, T. N.; Bourne, P. E.; Feng, Z. K.; Gilliland, G.; Weissig, H.; Westbrook, J. *Nat. Struct. Biol.* **2000**, *7*, 957.

(8) Hayward, S. *Normal-Mode Analysis of Biological Molecules*; Marcel Dekker Inc.: New York, 2001.

(9) Singwi, K. S.; Sjolander, a. *Phys. Rev.* **1960**, *120*, 1093.

(10) Rai, B. K. Dynamics of Iron Active Sites in Heme Proteins and Model Compounds. PhD thesis, Purdue University, 2003.

(11) Paulsen, H.; Winkler, H.; Trautwein, A. X.; Grunsteudel, H.; Rusanov, V.; Toftlund, H. *Phys. Rev. B* **1999**, *59*, 975.

(12) Sage, J. T.; Durbin, S. M.; Sturhahn, W.; Wharton, D. C.; Champion, P. M.; Hession, P.; Sutter, J.; Alp, E. E. *Phys. Rev. Lett.* **2001**, *86*, 4966.

(13) Sturhahn, W. *Hyperfine Interact.* **2000**, *125*, 149.

(14) Seto, M.; Yoda, Y.; Kikuta, S.; Zhang, X. W.; Ando, M. *Phys. Rev. Lett.* **1995**, *74*, 3828.

(15) Sturhahn, W.; Toellner, T. S.; Alp, E. E.; Zhang, X.; Ando, M.; Yoda, Y.; Kikuta, S.; Seto, M.; Kimball, C. W.; Dabrowski, B. *Phys. Rev. Lett.* **1995**, *74*, 3832.

(16) Sturhahn, W. *J. Phys.*: *Condens. Matter* **2004**, *16*, S497.

(17) Sturhahn, W.; Alp, E. E.; Toellner, T. S.; Hession, P.; Hu, M.; Sutter, J. *Hyperfine Interacti.* **1998**, *113*, 47.

(18) Achterhold, K.; Keppler, C.; Ostermann, A.; van Burck, U.; Sturhahn, W.; Alp, E. E.; Parak, F. G. *Phys. Rev. E* **2002**, 65.

(19) Achterhold, K.; Sturhahn, W.; Alp, E. E.; Parak, F. G. *Hyperfine Interact.* **2002**, *141*, 3.

(20) Alp, E. E.; Sturhahn, W.; Toellner, T. S. *J. Phys.*: *Condens. Matter* **2001**, *13*, 7645.

(21) Alp, E. E.; Sturhahn, W.; Toellner, T. S.; Zhao, J.; Hu, M.; Brown, D. E. *Hyperfine Interact.* **2002**, *144*, 3.

(22) Scheidt, W. R.; Wyllie, G. R. A.; Ellison, M. K.; Sage, J. T.; Rai, B. K.; Durbin, S. M.; Sturhahn, W.; Alp, E. E. *J. Inorg. Biochem.* **2003**, *96*, 51.

(23) Hu, M. Y.; Sturhahn, W.; Toellner, T. S.; Hession, P. M.; Sutter, J. P.; Alp, E. E. *Nuclear Instruments & Methods in Physics Research Section A. Accelerators Spectrometers Detectors and Associated Equipment*; North Holland Physics Publishers: Amsterdam, 1999; Vol. 428, p 551.

(24) Toellner, T. S.; Hu, M. Y.; Sturhahn, W.; Quast, K.; Alp, E. E. *Appl. Phys. Lett.* **1997**, *71*, 2112.

(25) Lipkin, H. J. *Phys. Rev. B* **1995**, *52*, 10073.

(26) Cusack, S.; Doster, W. *Biophys. J.* **1990**, *58*, 243.

(27) Diehl, M.; Doster, W.; Petry, W.; Schober, H. *Biophys. J.* **1997**, *73*, 2726.

(28) Argade, P. V.; Sassaroli, M.; Rousseau, D. L.; Inubushi, T.; Ikedasaito, M.; Lapidot, a. *J. Am. Chem. Soc.* **1984**, *106*, 6593.

(29) Melchers, B.; Knapp, E. W.; Parak, F.; Cordone, L.; Cupane, A.; Leone, M. *Biophys. J.* **1996**, *70*, 2092.

(30) Chern, L.; Prohofsky, E. W. *Phys. Rev. E* **1993**, *47*, 4483.

(31) Prohofsky, E. W. *Statistical Mechanics and Stability of Macromolecules*; Cambridge University Press: Cambridge, 1995.

(32) Fermi, G. *Molecular Structures in Biology*; Oxford University Press: New York, 1993.

(33) Rai, B. K.; Durbin, S. M.; Prohofsky, E. W.; Sage, J. T.; Ellison, M. K.; Scheidt, W. R.; Sturhahn, W.; Alp, E. E. *Phys. Rev. E* **2002**, *66*.

(34) Sage, J. T.; Paxson, C.; Wyllie, G. R. A.; Sturhahn, W.; Durbin, S. M.; Champion, P. M.; Alp, E. E.; Scheidt, W. R. *J. Phys.*: *Condens. Matter* **2001**, *13*, 7707.

(35) Rai, B. K.; Durbin, S. M.; Prohofsky, E. W.; Sage, J. T.; Wyllie, G. R. A.; Scheidt, W. R.; Sturhahn, W.; Alp, E. E. *Biophys. J.* **2002**, *82*, 2951.

(36) Rai, B. K.; Durbin, S. M.; Prohofsky, E. W.; Sage, J. T.; Ellison, M. K.; Roth, A.; Scheidt, W. R.; Sturhahn, W.; Alp, E. E. *J. Am. Chem. Soc.* **2003**, *125*, 6927.

(37) Guilbert, C.; Perahia, D.; Mouawad, L. *Comput. Phys. Commun.* **1995**, *91*, 263.

(38) Perahia, D.; Mouawad, L. *Comput. Chem.* **1995**, *19*, 241.

(39) Mouawad, L.; Perahia, D. *J. Mol. Biol.* **1996**, *258*, 393.

(40) Krebs, W. G.; Alexandrov, V.; Wilson, C. A.; Echols, N.; Yu, H. Y.; Gerstein, M. *Proteins*: *Struct., Funct., Genet.* **2002**, *48*, 682.

(41) Seno, Y.; Go, N. *J. Mol. Biol.* **1990**, *216*, 111.